Ab initio modeling of Molecular Radiation

Richard Jaffe
Aerothermodynanmics Branch
NASA Ames Research Center
Moffett Field, California 94035

Radiative emission from excited states of atoms and molecules can comprise a significant fraction of the total heat flux experienced by spacecraft during atmospheric entry at hypersonic speeds. For spacecraft with ablating heat shields, some of this radiative flux can be absorbed by molecular constituents in the boundary layer that are formed by the ablation process. Ab initio quantum mechanical calculations are carried out to predict the strengths of these emission and absorption processes. This talk will describe the methods used in these calculations using, as examples, the 4^{th} positive emission bands of CO and the $^1\Sigma_g^+ \rightarrow {}^1\Sigma_u^+$ absorption in C_3. The results of these calculations are being used as input to NASA radiation modeling codes like NeqAir, HARA and HyperRad.

Ab Initio Modeling of Molecular Radiation

Richard L. Jaffe and David W. Schwenke

NASA Ames Research Center

Moffett Field, CA 94035

STO-VKI Lectures on Radiation and Gas-Surface Interaction Phenomena in High Speed Re-Entry

University of Illinois at Urbana Champaign

April 7-9, 2014

Introduction

- **Modeling radiative heat flux fo hypersonic flight (~10 km/s, 50-90 km altitude)**
  - **Spectroscopic databases needed for NASA's existing radiation codes (NEQAIR, HARA) and new codes under development (e.g., HyperRad)**
  - **These codes use computed flow fields to predict radiative transport in the shock and boundary layer during re-entry**
  - **Validation using ground facilities (EAST, LENSxx, X3)**
  - **Ultimate goal: accurate prediction of heat flux on space vehicles during re-entry in order to reduce safety margins on thermal protection system**

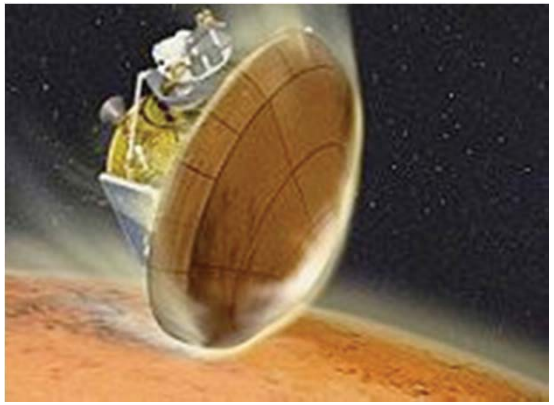

Re-Entry Conditions

- **Earth (N_2/O_2)**
  - **Hypervelocity return (> 9 km/s)**
  - **Large blunt bodies (several meter diameter)**
  - **Ablating heat shields (carbonaceous species injected into boundary layer)**
- **Mars (CO_2/N_2)**
  - **~6-8 km/s**
  - **MSL-size bodies and larger**
  - **Aerobraking at high altitudes (large flexible heat shield)**
  - **Conventional heat shields at lower altitude and speed**

Important radiative processes

- **Most radiation is from atomic emission (neutrals and cations)**
- **Strongest molecular emission from VUV bands**
  - **Much of this is re-absorbed by shock and boundary layer species before it reaches spacecraft surface**
- **Also contributions from bound-free and free-free continuum radiation (not within the scope of this presentation)**

Molecular Species of Interest

- **Earth**
  - **N_2, O_2, NO, N_2^+, NO^+ (emission in shock layer)**
  - **C_2, CO, C_2H, C_3H, C_3, C_4, etc. (absorption in boundary layer)**
- **Mars**
  - **CO_2 (IR), CO (IR, VUV), CN (UV-Vis), N_2 (UV)**

Spectroscopy: Top down or Bottom up?

The Old Way

- Start with experimental spectrum
- Determine initial and final ro-vibrational levels
  - Compute RKR potentials
  - Franck Condon factors
- Measure absolute (or relative) intensities of individual lines
  - Compute R-centroids
- Compute Einstein A-coefficients

The New Way

- Quantum mechanics all the way!
- Electronic Schrödinger equation
  - Compute potential energy curves (surfaces)
  - Compute transition moments and coupling terms
  - Obtain analytic fits
- Nuclear Schrödinger equation
  - Compute ro-vibrational levels
- Direct determination of Einstein A-coefficients

Quantum Mechanics Refresher

- **Electronic Schrödinger equation (clamped nuclei, shown for diatomic molecules)**

$$\left[-\frac{\hbar^2}{2m}\nabla^2 + V(\mathbf{r}) \right] u(\mathbf{r}) = E u(\mathbf{r})$$

- **V (potential)**
  - **electron-electron and electron-nucleus Coulomb interaction for potential energy calculations**
  - **diatomic potentials or triatomic PES for ro-vibrational energy level calculations**
- **Wavefunctions (u) and energy (E) determined by basis set expansion methods**

Spectroscopic intensity factors

- **Franck-Condon factors and R-centroids**

$$q_{v'v''} = \left[\int \psi_{v'}^{*} \, \psi_{v''} \, dr \right]^2$$

$$\bar{r}_{v'v''} = \int \psi_{v'}^{*} \, r \, \psi_{v''} \, dr \Big/ \int \psi_{v'}^{*} \, \psi_{v''} \, dr$$

- **Einstein A coefficient for spontaneous emission**

$$A_{v'v''} = (2.026 \times 10^{-6}) \frac{(2 - \delta_{0,\Lambda' + \Lambda''})}{(2 - \delta_{0,\Lambda'})} \nu_{v'v''}^{3} \left[\int \psi_{v'}^{*} R_e(r) \psi_{v''} dr \right]^2$$

- **$A_{v',v''}$ is the probability per unit time that a molecule in the upper state will decay to the lower state by emitting a photon**

Our Objective

- **Use quantum mechanical calculations to simulate molecular spectra from the IR to the VUV**
  - **Diatomic and triatomic molecules**
  - **Minimize empirical adjustments**
  - **Complete set of initial and final ro-vibrational levels**
  - **Electric and magnetic dipole and quadrapole transitions**
  - **Weak and strong band systems**
- **Simulate absorption and emission spectra for high-speed re-entry conditions**

New Wrinkles in the Present Work

- **Diatomic potentials accurate all the way to the dissociation limit *(not true for RKR and Morse-type potentials)***
- **Potentials include proper interactions due to coupling with other electronic states (e.g., spin orbit)**
- **Diabatic representation (instead of adiabatic) removes 'avoided crossings' by allowing states to cross**
- **Improved treatment for Rydberg states (cause of many of the avoided crossings)**

Avoided crossings

- **Adiabatic representation**
  - **diatomic potentials and PESs of same multiplicity and symmetry do not intersect as the red and green curves (top) illustrate**
  - **Avoided crossing results in change of electronic structure as shown by oscillator strengths (bottom)**

C_3 6 ^{1}A', 7 ^{1}A' & 8 ^{1}A' states

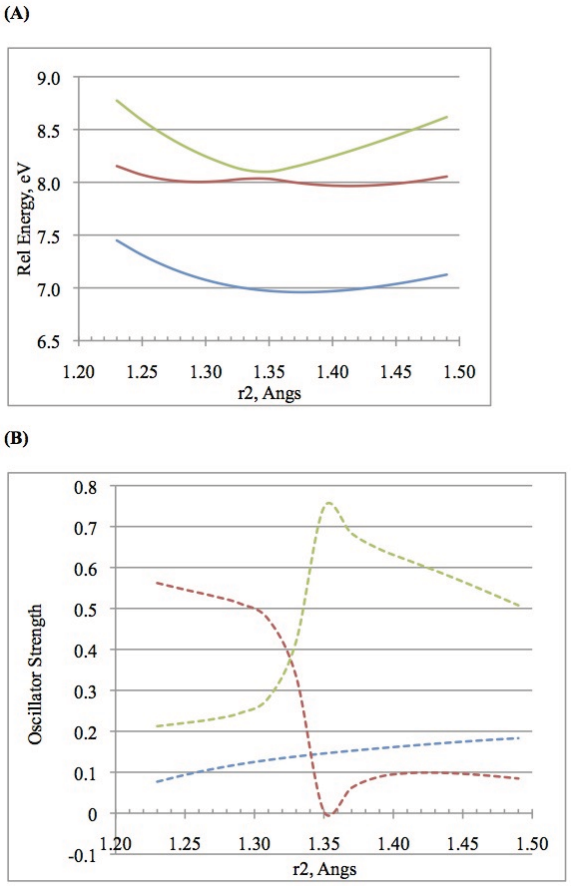

Diabatic representation

- **Adiabatic representation**
  - **Electronic states of same symmetry do not cross**
  - **But electronic structure of a state changes abruptly at geometries where two states are nearly degenerate (avoided crossing)**
- **Diabatic representation**
  - **Electronic structure of each state changes gradually as the geometry changes**

Adiabatic-diabatic transformation

- **Transformation effected by nuclear kinetic energy operator**
  - **Two-state example:**

$$T_{\mathrm{n}} = \sum_{A} \sum_{\alpha=x,y,z} \frac{P_{A\alpha} P_{A\alpha}}{2M_A} \quad \text{with} \quad P_{A\alpha} = -i\nabla_{A\alpha} \equiv -i\frac{\partial}{\partial R_{A\alpha}}.$$

$$\mathrm{T_n}(\mathbf{R})_{k'k} \equiv \langle \chi_{k'} | T_n | \chi_k \rangle_{(\mathbf{r})} = \delta_{k'k} T_{\mathrm{n}} + \sum_{A,\alpha} \frac{1}{M_A} \langle \chi_{k'} | \left(P_{A\alpha} \chi_k \right) \rangle_{(\mathbf{r})} P_{A\alpha} + \langle \chi_{k'} | \left(T_{\mathrm{n}} \chi_k \right) \rangle_{(\mathbf{r})}.$$

$$\begin{pmatrix} E_1(\mathbf{R}) + \mathrm{T_n}(\mathbf{R})_{11} & \mathrm{T_n}(\mathbf{R})_{12} \\ \mathrm{T_n}(\mathbf{R})_{21} & E_2(\mathbf{R}) + \mathrm{T_n}(\mathbf{R})_{22} \end{pmatrix} \mathbf{\Phi}(\mathbf{R}) = E\, \mathbf{\Phi}(\mathbf{R}) \quad \text{with} \quad \mathbf{\Phi}(\mathbf{R}) \equiv \begin{pmatrix} \Phi_1(\mathbf{R}) \\ \Phi_2(\mathbf{R}) \end{pmatrix}.$$

Adiabatic vs diabatic

- **Adiabatic**
  - **Easier to compute**
  - **Potentials are more accurate, but harder to use in calculations of ro-vibrational energy levels and spectra**
- **Diabatic**
  - **Harder to compute**
  - **Easier to use in subsequent calculations of molecular spectra**
  - **Requires more higher adiabatic states to have adequate convergence**
  - **Works well around potential minima, but not at the asymptotes**

Adiabatic/Diabatic Example

- NO $^2\Pi$ electronic states
  - Avoided crossings removed in diabatic representation
  - N + O asymptote not well described

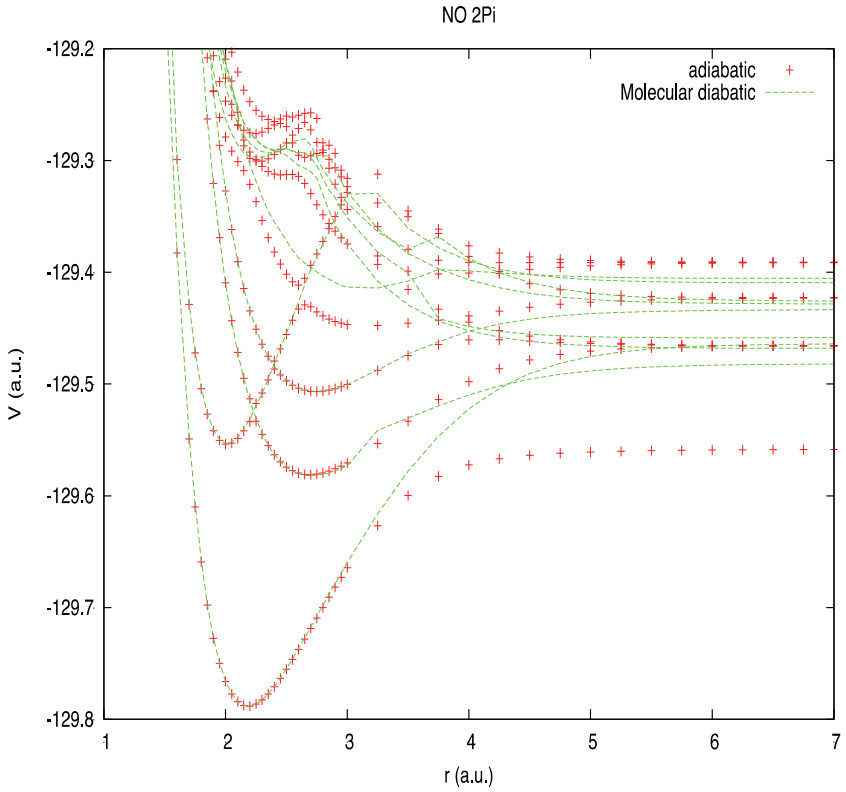

Difficulties computing VUV spectra

- **Typically there are many electronic states lying 6-12 eV above the ground state**
  - **This results in many avoided crossings (for states of the same symmetry and multiplicity)**
  - **Transitions with large oscillator strength are often spread among several upper electronic states (each one important for a small range or bond lengths or angles)**
  - **Hard to map out all of this and to fit these potentials and transition moments**

Difficulties for triatomic molecule calculations

- **Triatomic molecules have 3 geometric parameters**
  - **2 bond lengths and 1 bond angle**
  - **Many more energy calculations needed to represent 3-d potential hypersurface**
- **Linear triatomic molecules like CO_2 and C_3 have lower symmetry as they are distorted**
  - **$D_{\infty h}$ for 180° bond angle and equal bond lengths (Σ_g^+, Σ_u^+, Π_g, Π_u, etc.)**
  - **C_s for < 180° bond angle and unequal bond lengths (A', A")**

Examples today

- **CO 4th-positive emission**
  - **A $^1\Pi \rightarrow$ X $^1\Sigma^+$**
  - **0-0 transition at 154.4 nm**
  - **Typically observed in 145-195 nm wavelength range**
  - **Shorter wavelengths obscured by black body limit**
  - **Largest molecular contributor to radiative flux for Mars entry**
- **C_3 VUV absorption**
  - **$^1\Sigma_u^+ \leftarrow$ X $^1\Sigma_g^+$**
  - **0-0 transition between 160-170 nm**
  - **Overlaps very strong N(I) lines at 174.27 and 174.52 nm**

CO 4+: Computed electronic state potentials

- **Transition between CO A $^1\Pi$ and ground state (X $^1\Sigma^+$) [lines with symbols]**
  - **Four triplet states perturb the A state potential**
  - **Three Rydberg states shown [dashed lines]**
- **0-0 transition at 154.4 nm (64,748.48 cm^{-1})**

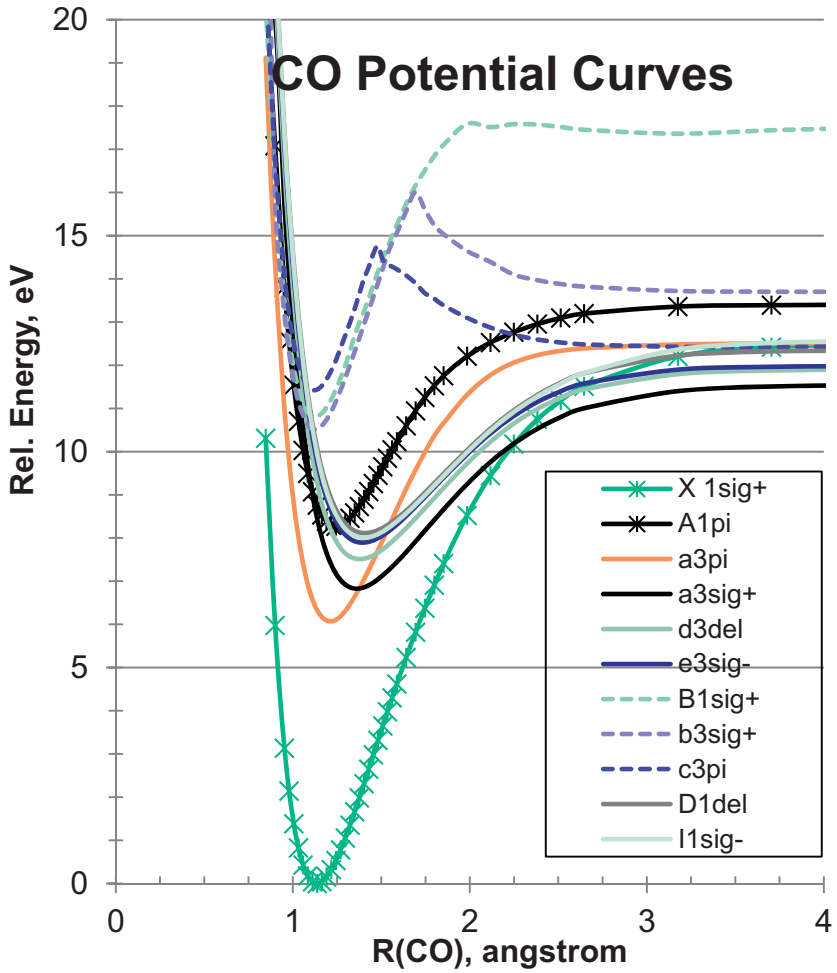

CO 4+

- **This transition accounts for more than 60% of the integrated radiative flux for typical Mars entry at 8 km/s**

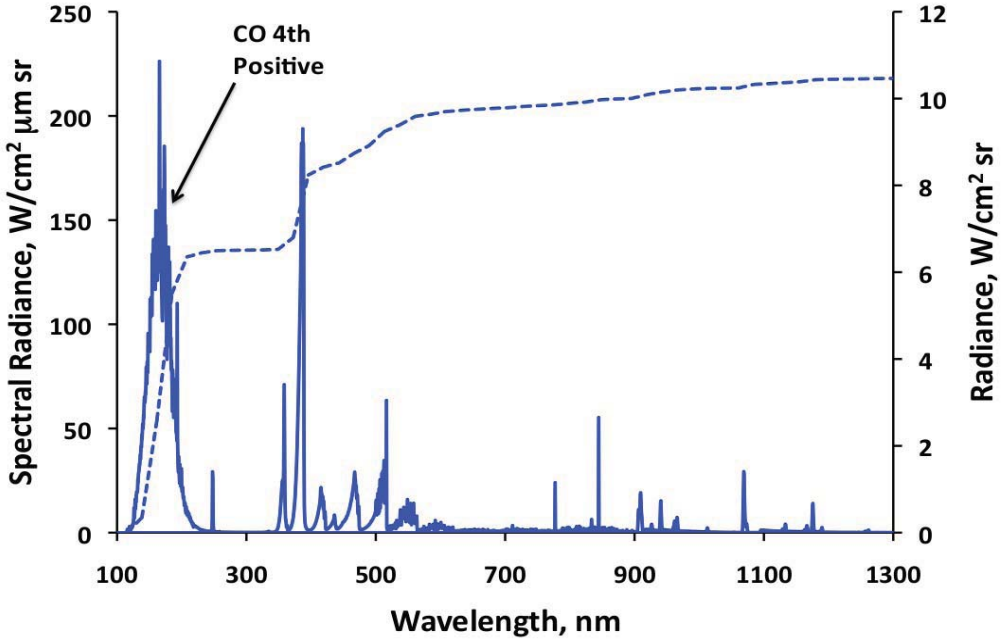

CO 4+ Comparison

- **Measured in EAST facility at NASA Ames (Electric Arc Shock Tube) – pure CO_2 at 6.3 - 8 km/s**
- **Simulation by NEQAIR (vintage code with current *top-down* spectral database) and HyperRad (new code with new *bottom-up* database)**
- **Measured instrumental width applied with natural line broadening factors**

A $^1\Pi$ potential curve shifted up by 0.013 eV (105 cm^{-1}) to match experimental T_e

Comparison of Spectral Databases

Red curved line is black body cutoff for 6085 K

Shock speed is 6.3 km/s

0-0 transition marked by arrow

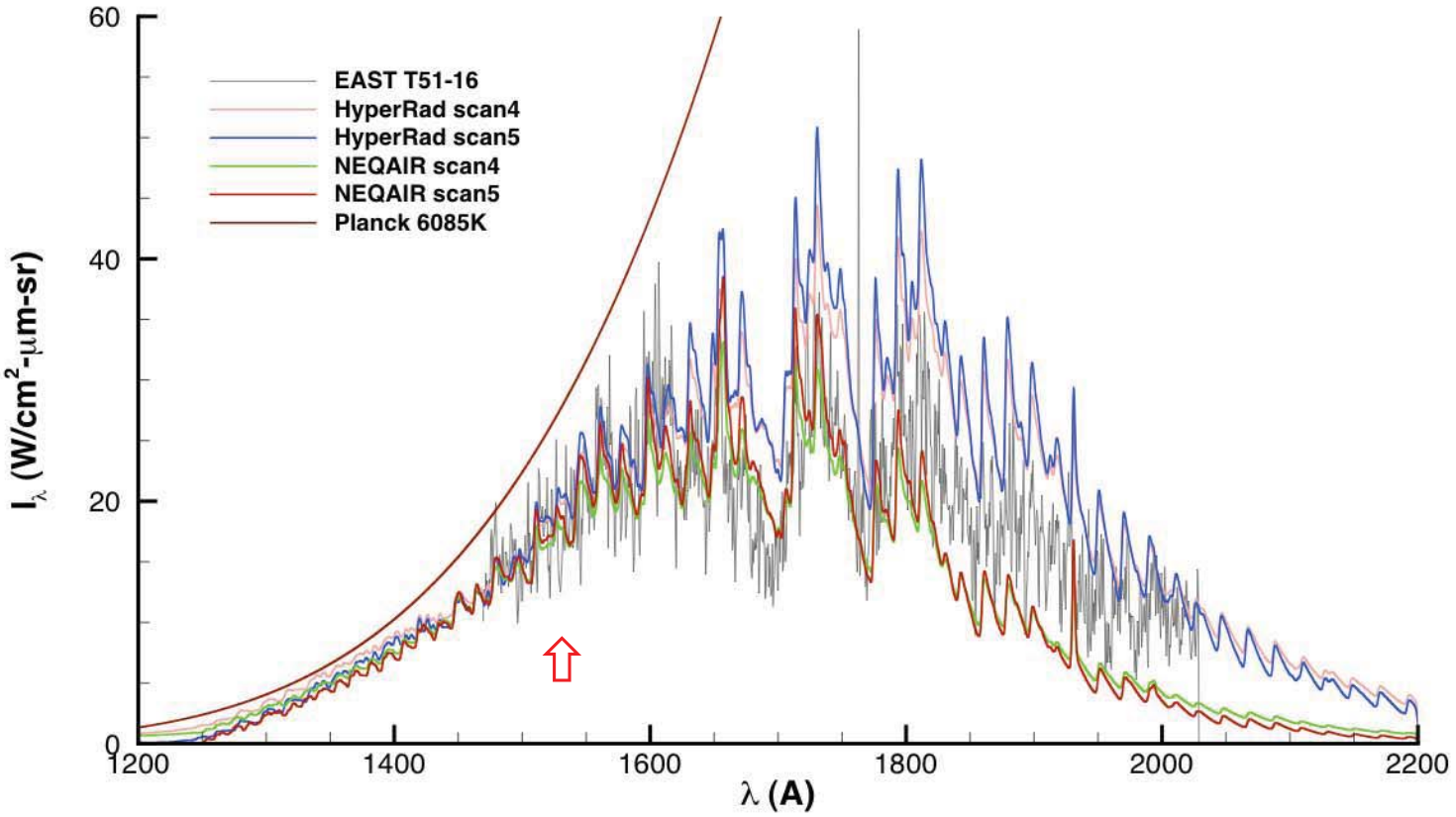

CO 4+ wrap up

- **State-of-the-art quantum mechanical calculations can predict ro-vibrational energies to within 10 cm-1 and electronic excitation energies to ~100 cm-1 (~0.01 eV)**
  - **Spectroscopic measurements still better for obtaining precise wavelengths of spectral lines**
  - **Simple adjustment of of T_e values for electronic states can yield accurate spectra**
- **For the CO 4+ transition new database has very good match to EAST measurement**
  - **Old experiment-based database comparable at shorter wavelengths, but errors grow for longer wavelengths (higher ground state rovibrational levels)**

C_3 spectroscopy

- C_3 is the most stable carbon molecule in the vapor phase
  - Product of arc heated graphite and shocked acetylene or methane
  - Linear molecule with very small bend frequency
- Vis-UV spectral bands (Swings) from $^1\Pi_u \rightarrow {}^1\Sigma_g^+$ transition observed in emission and absorption
- Poorly characterized VUV absorption transition due to $^1\Sigma_u^+ \leftarrow {}^1\Sigma_g^+$
- Injected into the boundary layer during re-entry as a pyrolysis product of ablating heat shields

Role of C_3 during re-entry

- **Boundary layer C_3 could absorb some of the incident radiative heat flux originating in the shock layer**
  - **Pair of very strong atomic nitrogen lines at 174.27 and 174.52 nm lie within the wavelength range of this feature**
  - **High-resolution spectrum only observed at T < 10 K (Monninger et al., J Phys Chem A 2002, 106, 5779)**
  - **Possible feature seen in high-temperature shock tube experiment (Shinn AIAA-1982-1189)**
- **Objective – characterize C_3 VUV feature for T ~ 3000 K and assess its 'radiation blocking' potential**

C_3 Experimental Low-T Spectra

- **Monninger et al. absorption spectra**
  - **Upper 10 K in solid Ar**
  - **Lower 4.3 K in solid Ne**
- **Peak intensity 160-170 nm**
  - **Band extends from ~145-180 nm**
- **C_3 generated from arc-heated graphite and trapped in cryogenic matrix**

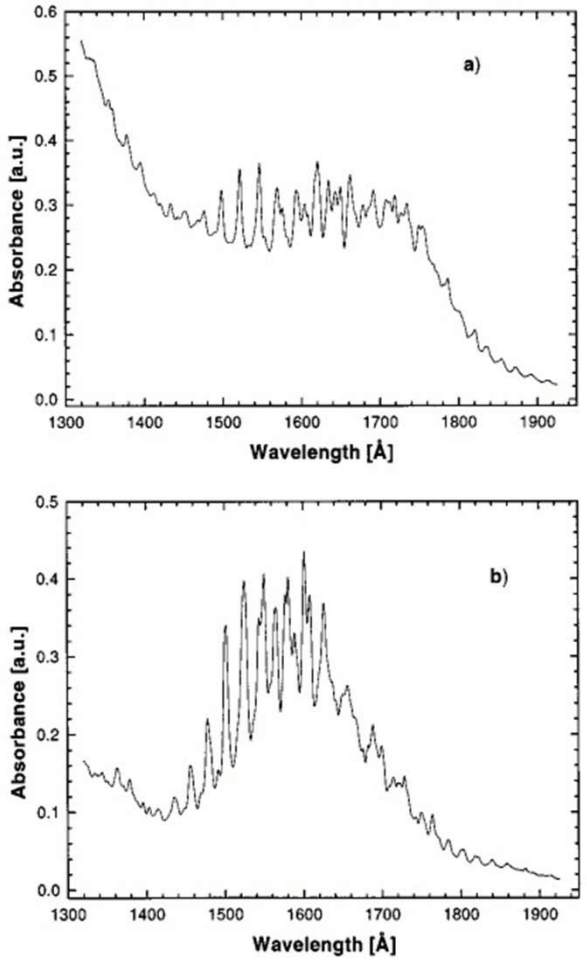

Figure 4. Absorption spectra of the C_3 ($^1\Sigma^+_u - X\ ^1\Sigma^+_g$) system (a) in solid argon at 10 K and (b) in solid neon at 4.3 K. The spectra are recorded at a resolution of 1 Å, and no background correction was applied.

Experimental High-T Spectra

- **Shinn (NASA Langley) 1% C2H2 or 2% CH4 in Ar in shock tube at T = 3600-4100 K**

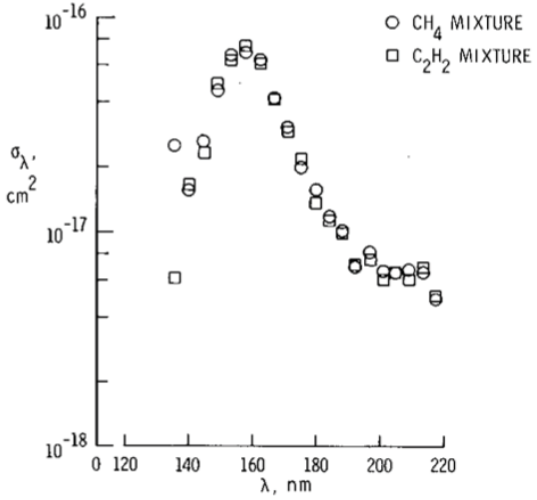

Fig. 6 Comparison of C_3 cross section measured at temperature 3650-3850 K range using 1-percent C_2H_2 plus 99-percent argon mixture and 2-percent CH_4 plus 98-percent argon mixture.

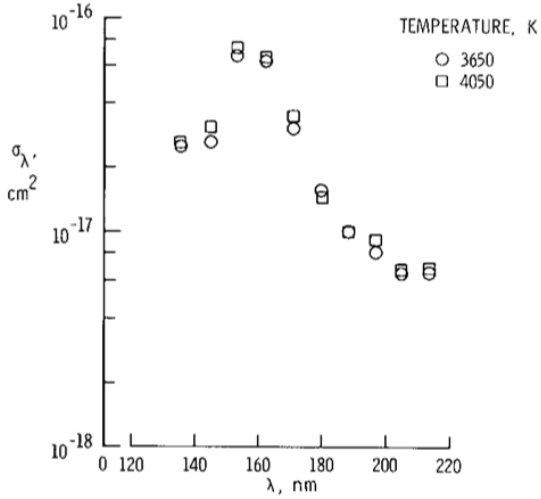

Fig. 8 Comparison of C_3 absorption cross section between tests performed at two different temperatures with a mixture of 2-percent CH_4 plus 98-percent argon.

C_3 ground electronic state

- **Very small bending frequency (ω_e = 63.4 cm^{-1})**
  - **Large bend amplitude (± 60°)**
- **At cryogenic temperatures, only the lowest rovibrational energy level is populated**
- **At 3000 K (typical boundary layer temperature) hundreds of ro-vibrational levels are populated**
  - **Lowest level accounts for ~2% of the total population**

Contour plot of ground state PES in terms of bending and symmetric stretch

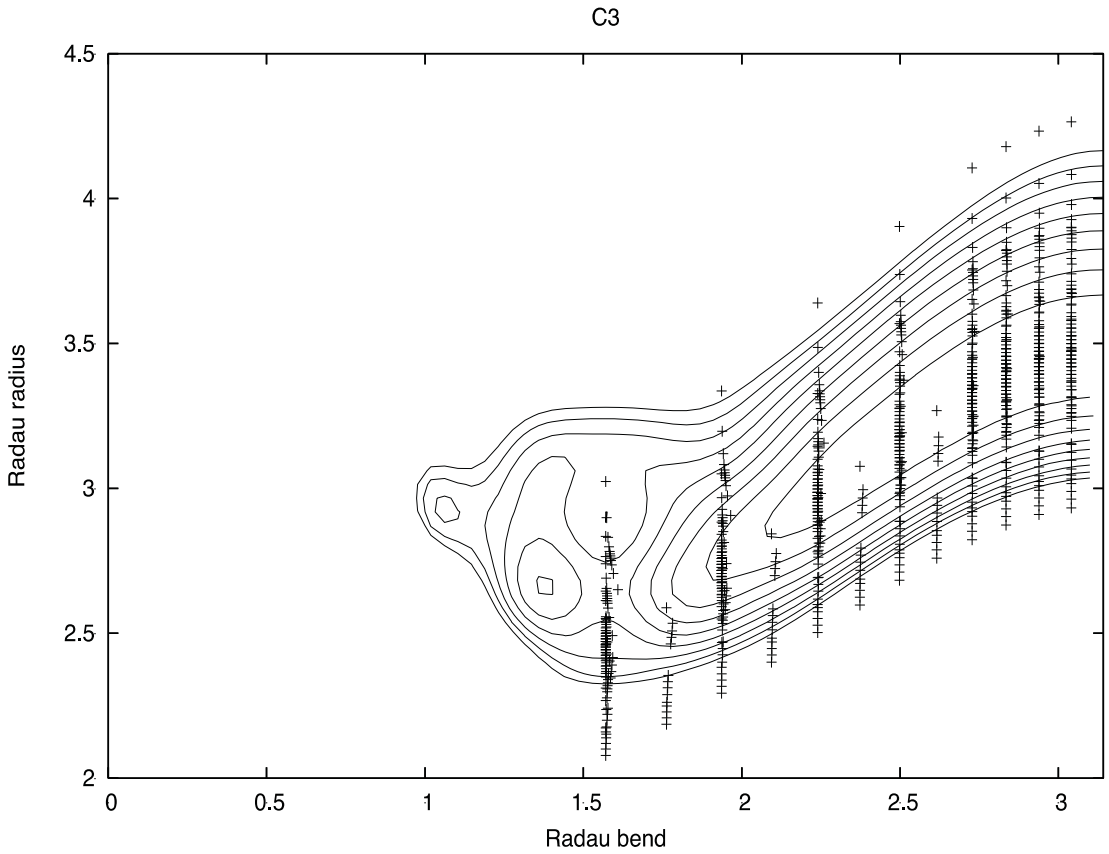

C_3 Bending potential and energy levels

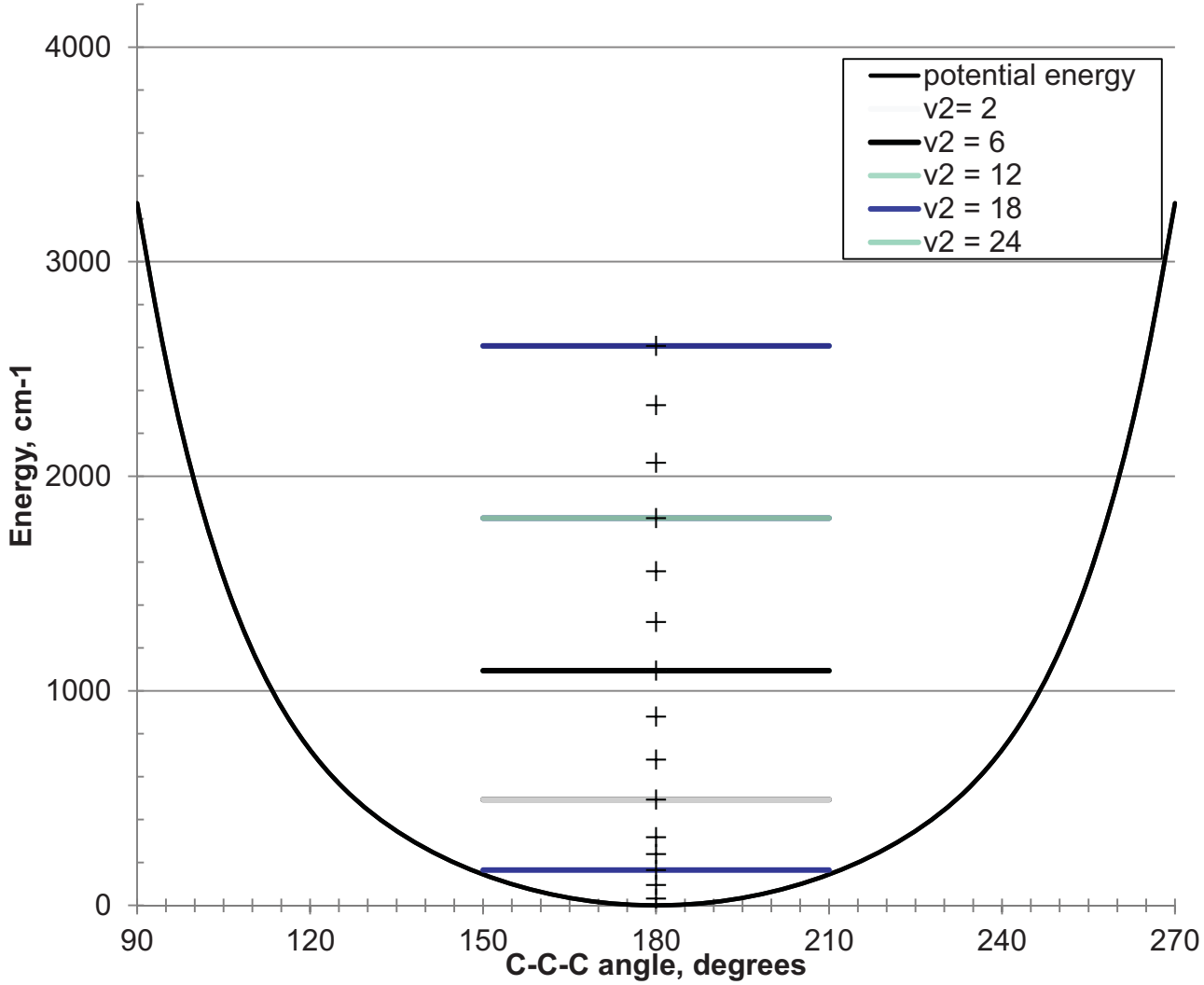

C_3 excited electronic state potentials

- **Next two slides show C_3 excited electronic states in terms of the bending and asymmetric stretch coordinates**
- **The VUV transition involves states that are 6-8 eV above the ground electronic state**
- **The Swings bands (vis-UV) involves the lowest excited state ($^1\Pi_u$ which becomes 2 ^{1}A' + 1 ^{1}A" at non-linear geometry)**
  - **Splitting due to Renner-Teller coupling (blue solid and dashed curves)**

C_3 bend: adiabatic vs diabatic

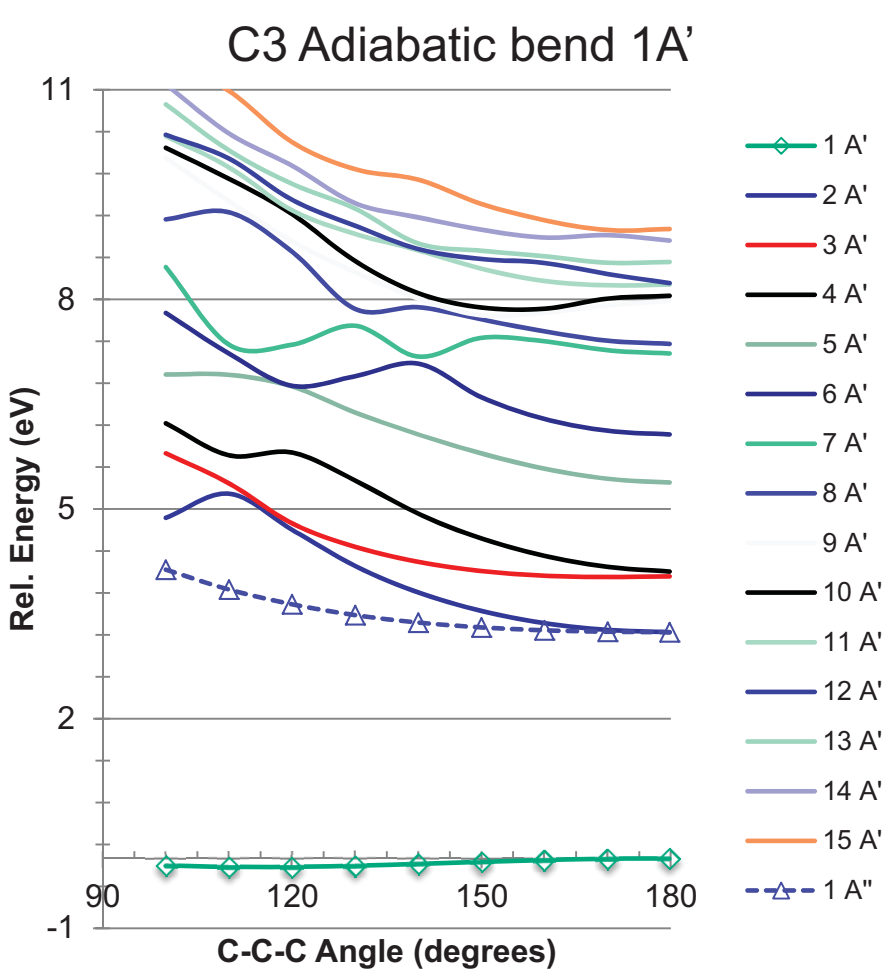

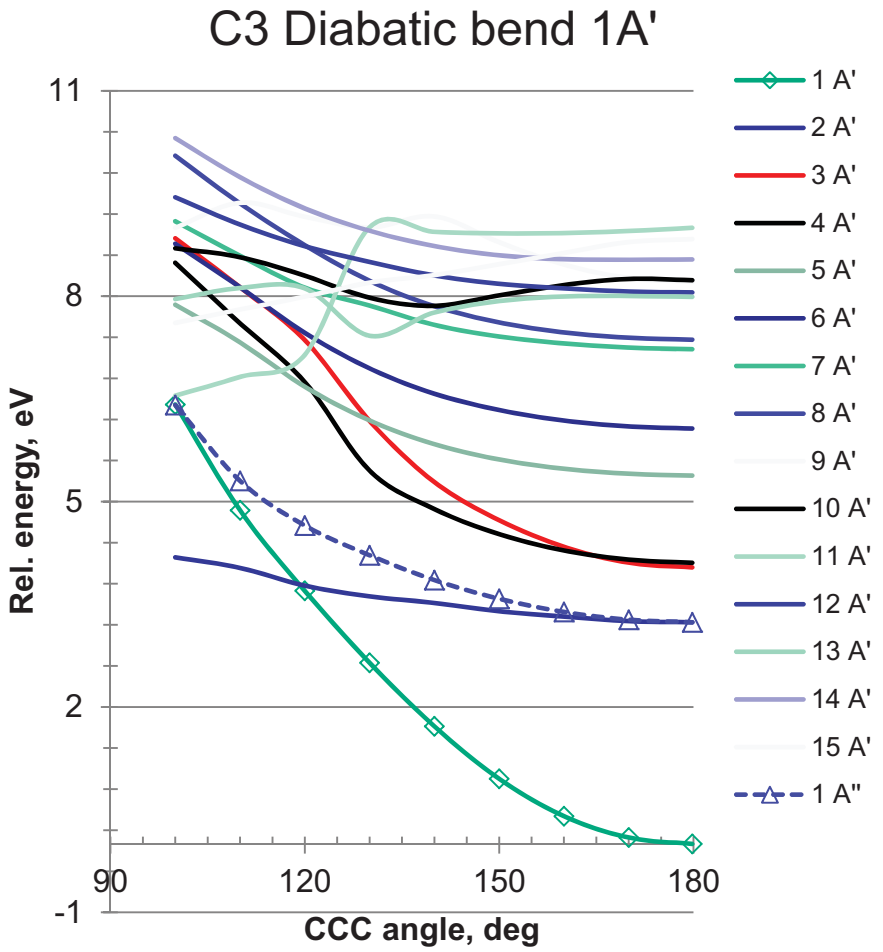

C_3 asymmetric stretch: adiabatic vs diabatic

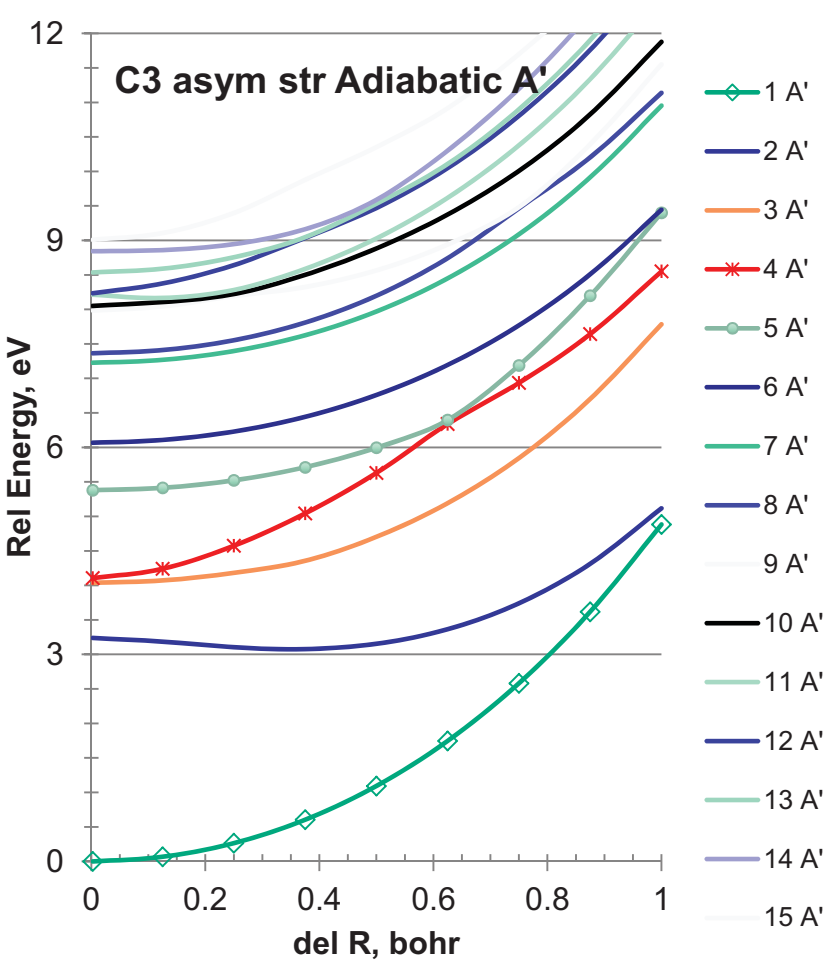

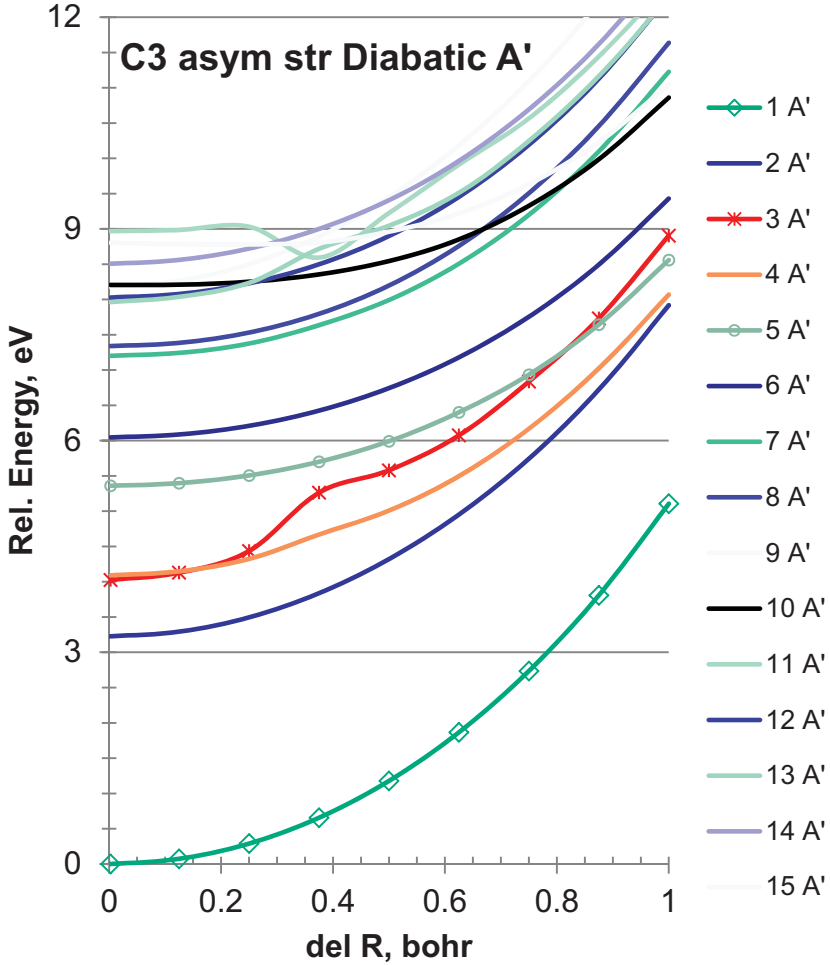

Computed and observed 4.3 K spectra

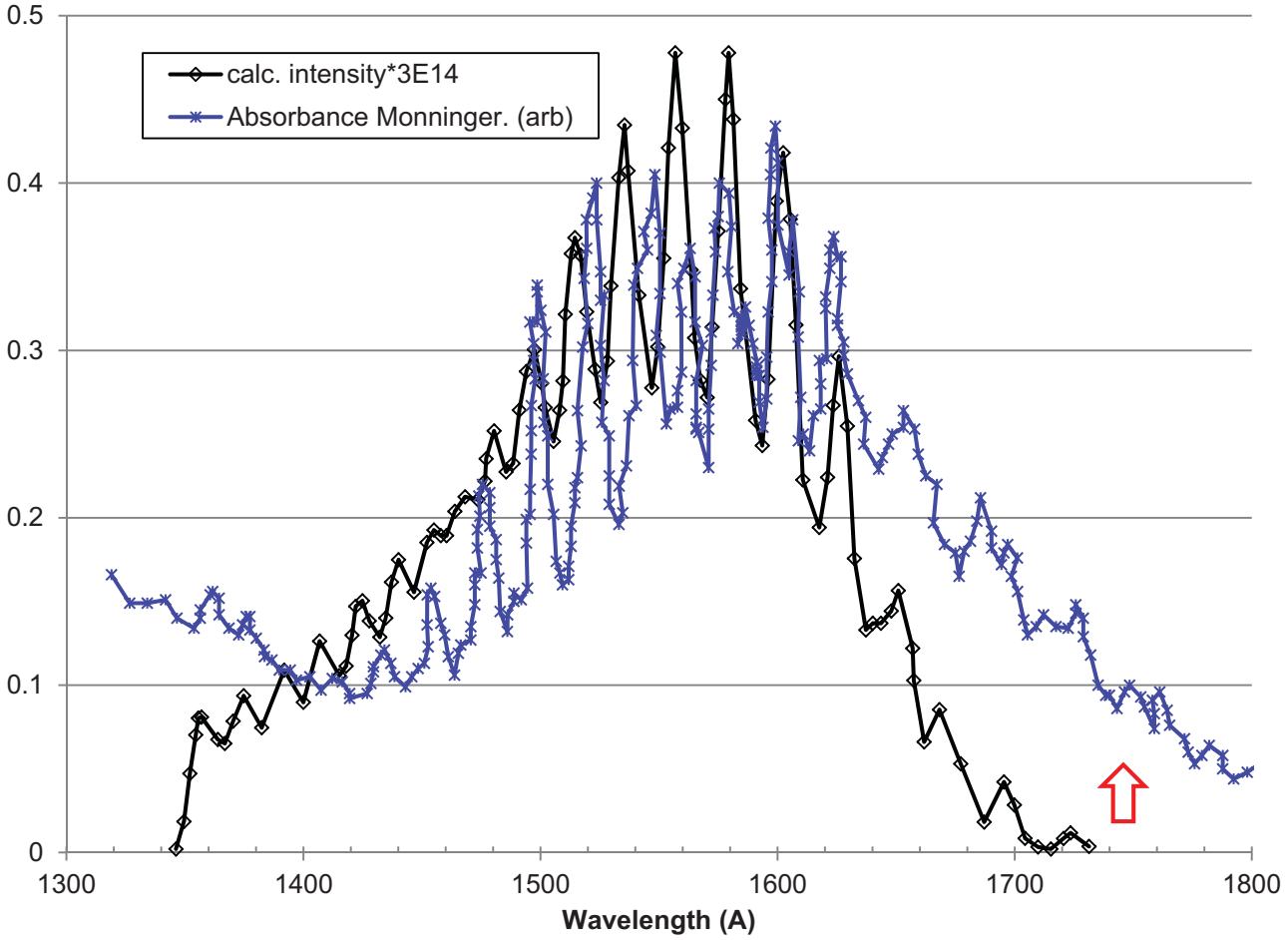

⇧

C_3 VUV spectrum at 3000 K

PRELIMINARY RESULT

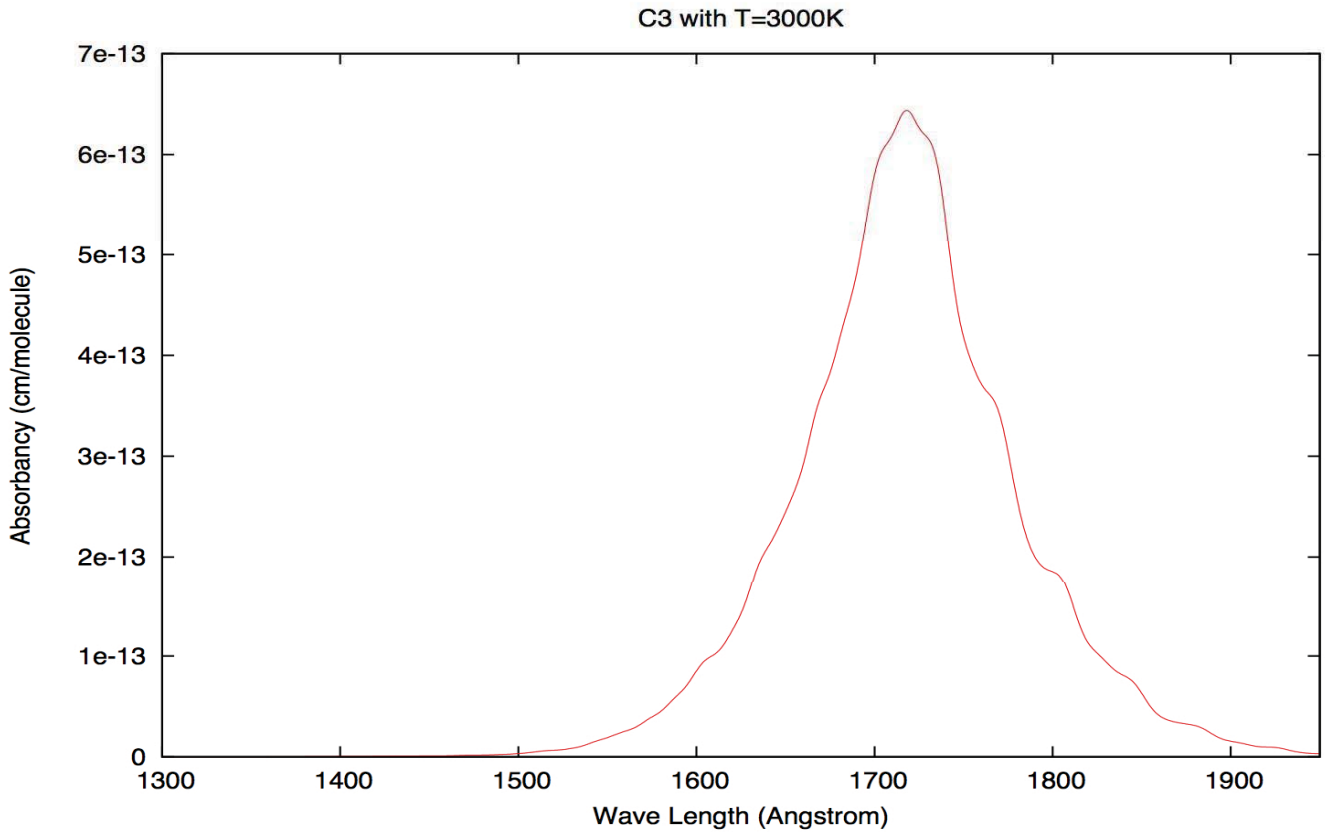

Shape consistent with Shinn spectra, but red-shifted

C_3 wrap up

- **Computed cryogenic and 3000 K absorption spectra for C3 VUV transition**
  - **At low temperature the computed spectrum agrees well with experimental result of Monninger et al**
  - **At high temperature the computed spectrum has the same shape as the result from Shinn's shock tube experiments, but the peak is red shifted to 172 nm**
- **The population of many ground state ro-vibrational levels washes out structure seen in the 4.3 K spectrum**
  - **Peak in absorption spectrum is red shifted at high temperatures due greater contribution from higher ground state ro-vibrational levels**

Supports hypothesis that C_3 VUV can absorb N 174 nm

Gallery of Computed Diatomic spectra: CO

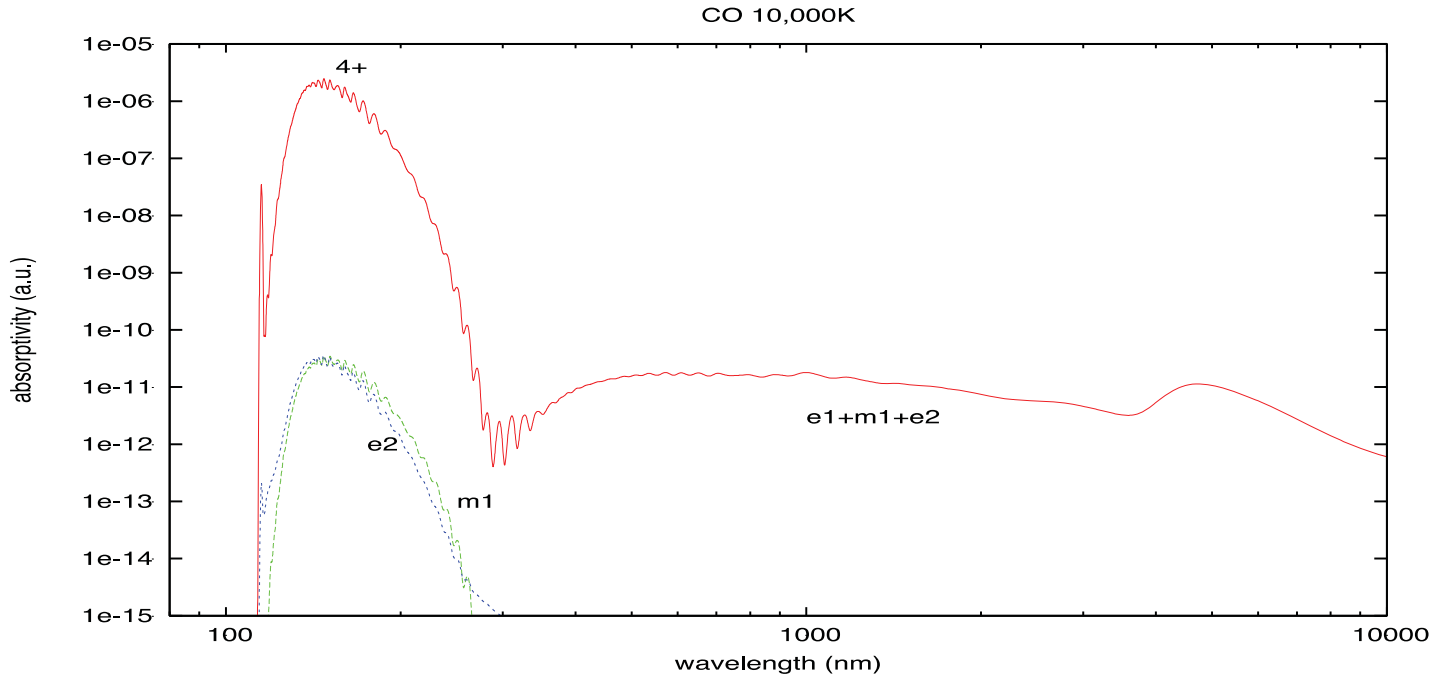

e1 = electric dipole
e2 = electric quadrapole
m1 = magnetic dipole

Gallery of Diatomic spectra: CN & C_2

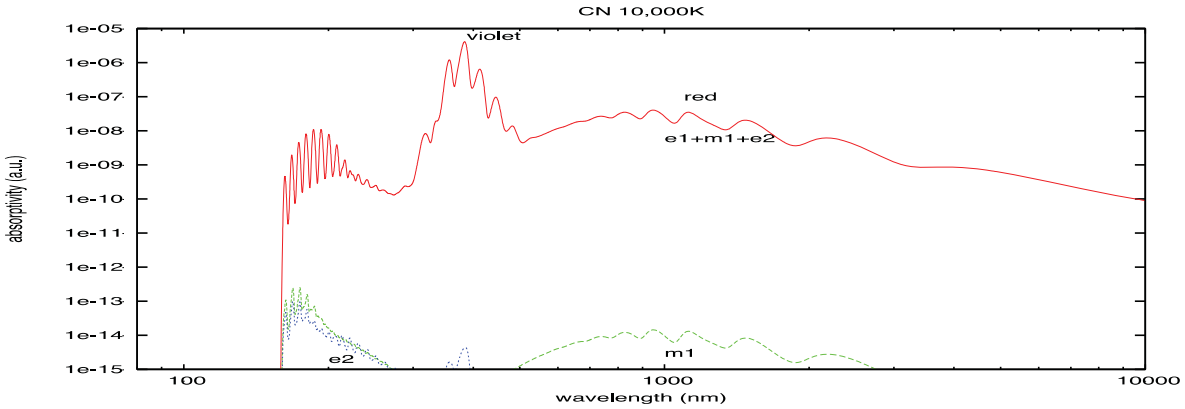

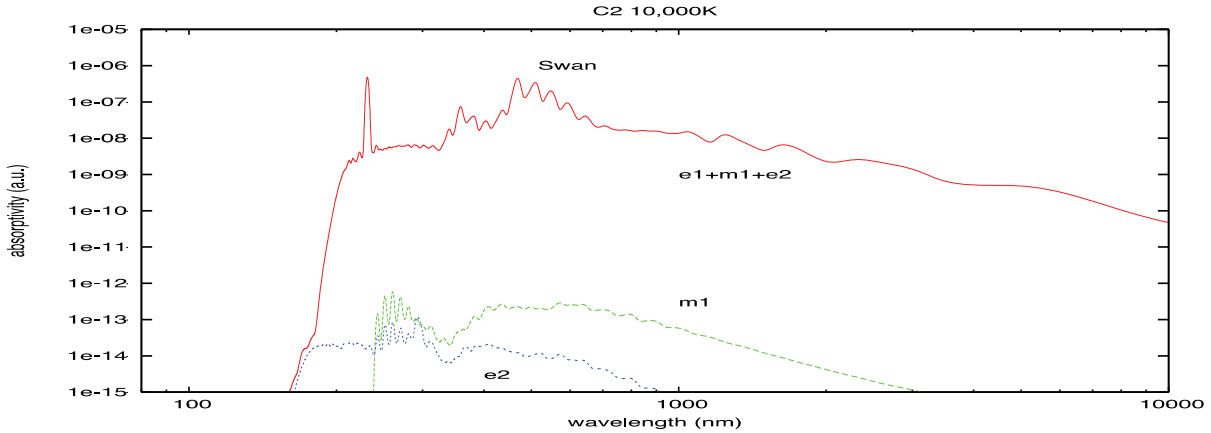

Gallery of Diatomic spectra: N2 & NO

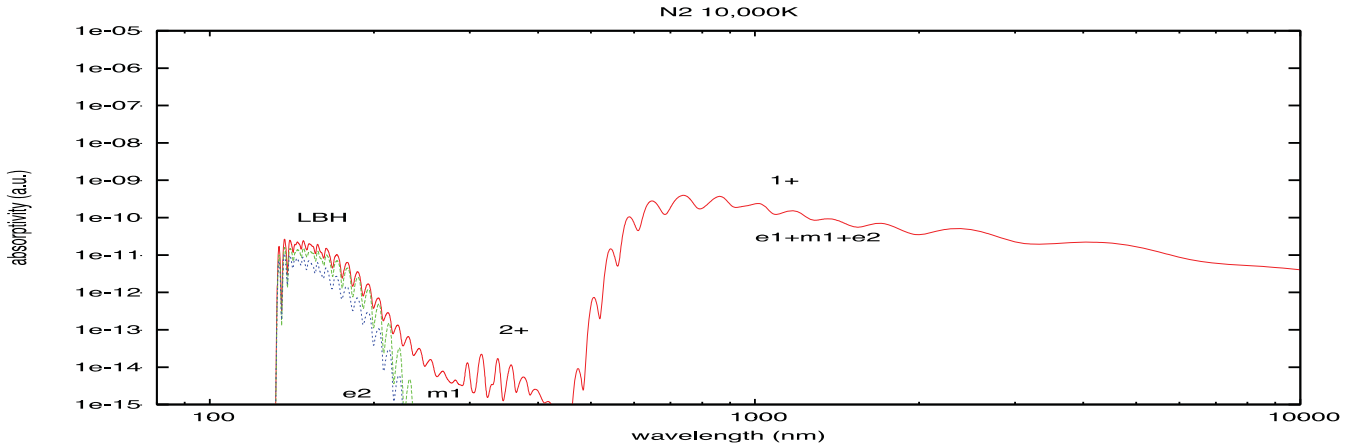

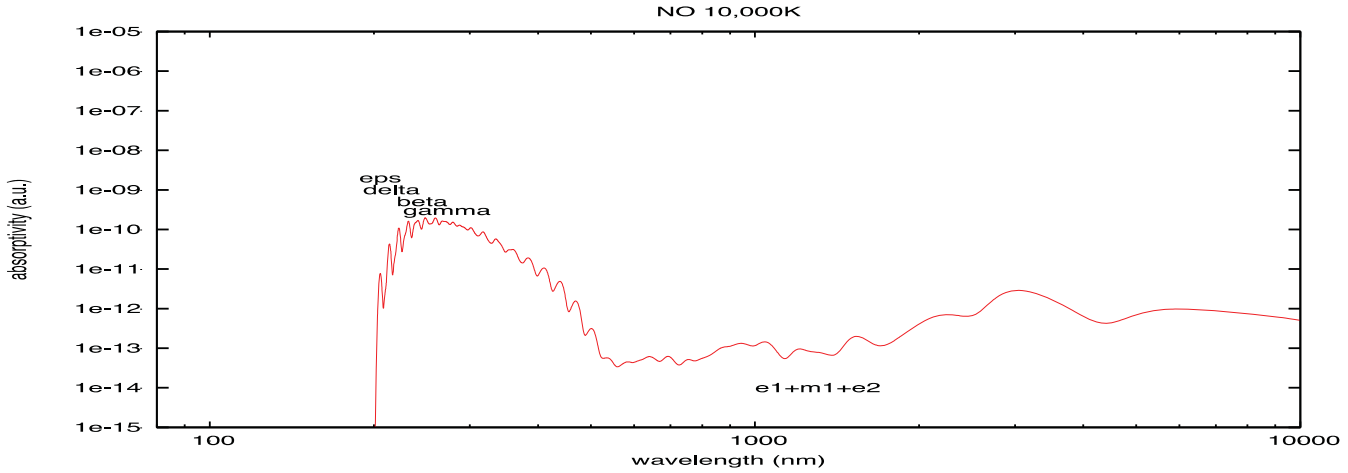

Summary

- **Bottom-up quantum mechanical approach can yield accurate VUV spectra for diatomic and triatomic molecules at high temperatures**
- **Only small empirical adjustment of upper electronic state T_e values needed**
- **For CO 4+ the resulting spectra are in somewhat better agreement with spectra derived from EAST**
- **For C_3 resulting VUV spectra are much more accurate than anything previously available**
- **Results support hypothesis that C_3 VUV can absorb N 174 nm**

Final thoughts

Ab initio molecular VUV spectroscopy is competitive with traditional approaches for diatomics and represents a major advance when it comes to triatomics.

Studies should be carried out to assess the effectiveness of C_3 in blocking N 174 nm radiation.

Acknowledgements

- **Technical assistance from Winifred Huo, Galina Chaban, Yen Liu and Alan Wray (NASA Ames)**
- **Many helpful discussions with Dinesh Prabhu (Ames), Brett Cruden and Aaron Brandis (EAST facility at Ames) and Chris Johnston (NASA Langley)**
- **Support from the NASA Fundamental Aeronautics/Hypersonics program, Space Technology/Hypersonic-Entry Descent and Landing Project (now renamed Entry Systems Modeling)**